Magnetic-Induced Coil-Globule Transition for Polyelectrolytes

Bin Yuan, Linli He, Linxi Zhang

Department of Physics, Wenzhou University, Wenzhou 325035, People's Republic of China

Received 19 June 2011; accepted 6 January 2012
DOI 10.1002/app.36769
Published online in Wiley Online Library (wileyonlinelibrary.com).

ABSTRACT: The effects of an applied magnetic field on the system composed of polyelectrolytes (PEs) and magnetic nanoparticles oppositely charged are studied by means of Monte Carlo method within the framework of "single-site bond fluctuation model." For a certain concentration of chains, the coil-globule transition can be induced by the applied magnetic field. The mean-square end-to-end distance and gyration radius as well as the shape factor of PE chains are used to characterize the conformational transitions. The statistical analysis of the system energy demonstrates this significant physical process. The role of entropy-energy balance is well-understood for different chain lengths, and a typical phase-transition anomaly concerned with specific heat curve is observed. Under a certain magnetic field, the PE chains will regularly collapse due to the enough adsorption of magnetic particles. The magnetic particles exhibit peculiar spatial distribution at high magnetic fields: the string-like arrangement along the magnetic field and the square lattice-like arrangement perpendicular to the magnetic field. The applied magnetic field has a great influence on the length of string-like structures formed by nanoparticles. This investigation may cast light on the collapse of PEs and provide a promising method for producing new nanocomposites. © 2012 Wiley Periodicals, Inc. J Appl Polym Sci 000: 000–000, 2012

Key words: polyelectrolytes; magnetic nanoparticles; coil-globule transition; Monte Carlo method

INTRODUCTION

As is well known, the conformation behavior of polymer chains in solutions depends on solvent conditions. The chain conformation can changes from a coil state in good solvents to a globule state in poor solvents. Since its first experimental observation by Tanaka and coworkers,[1] the coil-globule transition has been the subject of theoretical and experimental studies to date. The great and lasting interest in this research area can be attributed to its qualitative similarity to protein folding, DNA condensing, and its application to many related fields, such as medicine and biotechnology. The coil-globule transition can be influenced or induced by various factors,[1–11] such as confinement, chain stiffness, hydrogen bond, and hydrodynamic interactions. Excellent studies on theories, experiments, and simulations can be found everywhere.[12,13] Additionally, there are two classical polymer physics books[14,15] where more details can be found.

The polyelectrolyte (PE) is the subsequent subject of great importance, because a large number of charged groups are commonly found among biological macromolecules, such as DNA and RNA. There is a competition between the electrostatic interactions and solvent conditions, which codetermines the conformational properties of PE chains. The size of PE chains is far larger than that of the uncharged one, due to the electrostatic repulsion among intrachain clusters. Furthermore, the PE size is closely related to the number of monomers. As for strongly charged PEs, an effective polymer charge screening and a decrease in polymer size occur, when the electrostatic energy of polymer-counterion attraction is larger than the corresponding loss of entropy due to the counterions in the close vicinity of the PEs in salt-free solutions.[16] The effect of salt concentration as well as the charge density of a single PE chain is pronounced. For instance, strongly charged flexible PEs collapse if the concentration of the salt exceeds a critical value, and re-expand while the second critical value is exceeded.[17] Muthukumar and coworkers found that the polyion chain already collected its counterions, when the dimensions started to shrink below the good solvent limit but still well above the θ-dimension.[18] On the other hand, as demonstrated by Panwar et al., who combined the single molecule force spectroscopy experiments with Langevin dynamics simulations,[19] the globule-coil transition was accompanied by a correlated counterion

Correspondence to: L. He (helinli155@163.com).
Contract grant sponsor: National Natural Science Foundation of China; contract grant numbers: 20774066, 20974081, 20934004, 21104060.
Contract grant sponsor: National Basic Research Program of China; contract grant number: 2005CB623800.

desorption, because the gain in mobile counterion entropy was greater than the chain-counterion adsorption energy. It is convincing that the attractive dipole–dipole interactions between chain monomers and counterions in their vicinity might lead to a collapse of highly charged PEs with counterions. The chain dimensions are a function of PE linear charge density in the limit of compacting chains.[20] Moreover, the coupling between the effective charge and polymer size plays a key role in the coil-globule transition of PEs in poor solvents.[21]

However, there are few reports considering the effects of external magnetic field on the conformational properties of PEs chain. Our work introduces a model system to study the effects of the applied magnetic field on the conformational properties of charged PEs polymers. Additionally, our previous works[22] has provided some good results consistent with the related experiment.[23] Although the logical and meaningful results have been obtained, it would be more reasonable if the long-range property of electrostatic interaction can be seriously considered. Thus, we extend the effective range of electrostatic interactions to consider the model system composed of PEs and magnetic nanoparticles, which is subjected to an applied magnetic field. Simply blending polymers and particles is the most commonly used way of nanocomposites syntheses.[24] The charged polymers are particularly useful matrices. Some thin film systems including PE multilayers can be good examples.[25–28] The properties of polymer nanocomposites strongly depend on the spatial arrangement of nanoparticles and the phase behavior of polymer chains. Then, the external magnetic field are used to orient polymers[29] with the inclusion of magnetic particles. The orderly polymer nanocomposites with a wide range of tunable properties can be obtained. In addition, microcapsules composed of PEs and nanoparticles can be moved or concentrated[30] by the magnetic field, which has a promising application in drug delivery. They can be used as the magnetic-sensitive nanocomposite microcapsule shell structure to regulate the release of drug in a manageable manner.[31] We expect that some conformational properties of system, such as the mean dimensions, would vary with the magnetic field monotonously. Our results confirm that the magnetic field has a great influence on the size of PE chains. For a certain concentration of PEs mixed with magnetic particles oppositely charged, the coil-globule transition is induced with increasing the applied magnetic field. In this article, we first focus on the dependence of the conformational properties on the applied magnetic field and then probe into the nature of the conformational transition. Finally, the effects of the applied magnetic field on the spatial arrangement of magnetic particles are investigated.

MODEL AND SIMULATION METHODS

Here, the Monte Carlo (MC) method is used to investigate the mixtures of PEs and magnetic nanoparticles. The linear polymer chain is composed of $N + 1$ monomers, which are restricted to the simple cubic lattices. The charges of the polymers are uniformly distributed among all the monomers. For simplicity, charge neutrality is maintained by introducing M magnetic nanoparticles with opposite and equal charges, where the particle size is the same as the monomer. This assumption is not absolute because the charge neutrality is maintained by counterions, but implies that the charges carried by magnetic nanoparticles are sufficient to affect the PEs' conformation. The magnitude of magnetic moment vectors for all particles are defined as $|\vec{m}_i| = m_0 = 1.0$ ($i = 1,2,\ldots,M$), and the direction of the initial magnetic moment vector is chosen to be random. Furthermore, the components of magnetic moment vectors $\vec{m}_i$ can be expressed as follows in the Cartesian coordinates:

$$\begin{aligned} m_{ix} &= m_0 \sin\theta_i \cos\phi_i = \sin\theta_i \cos\phi_i \\ m_{iy} &= m_0 \sin\theta_i \sin\phi_i = \sin\theta_i \sin\phi_i \\ m_{iz} &= m_0 \cos\theta_i = \cos\theta_i (i = 1, 2, \cdots, M) \end{aligned} \tag{1}$$

where θ_i represents the angle between the magnetic moment vector of ith magnetic nanoparticle and the direction of the applied magnetic field with $0 \le \theta_i \le \pi$, and ϕ_i is the azimuthal angle in the xy-plane from the x-axis with $0 \le \phi_i \le 2\pi$. The direction of the applied magnetic field H is defined along the z-axis in the Cartesian coordinate.

Thus, the total energy of system can be expressed as follows in the unit of kT, where k and T denote the Boltzmann constant and temperature, respectively:

$$E = E_m + E_e \tag{2}$$

where the magnetic energy E_m, including two parts: the field-particle interaction E_H imposed by the magnetic field and the magnetic dipole–dipole interaction E_D between magnetic nanoparticles, is expressed as follows:

$$\begin{aligned} E_m = &-\sum \vec{m}\vec{H} \\ &+ \frac{1}{4\pi\mu_0} \sum_i \sum_{j(j\neq i)} \left\{ \frac{\vec{m}_i \bullet \vec{m}_j}{r_{ij}^3} - \frac{3}{r_{ij}^5} (\vec{m}_i \bullet \vec{r}_{ij})(\vec{m}_j \bullet \vec{r}_{ij}) \right\} \end{aligned} \tag{3}$$

where r_{ij} is the distance between particles i and j, and H the magnitude of the applied magnetic field. For simplicity, $1/(4\pi\mu_0) = 1.0$ and $kT = 1.0$ are designed. The electrostatic energy E_e is defined in the following form:

$$E_e = n_{PP}\varepsilon_{PP} + n_{PN}\varepsilon_{PN} + n_{NN}\varepsilon_{NN}$$
$$E_{PP} = n_{PP}\varepsilon_{PP}, E_{PN} = n_{PN}\varepsilon_{PN}, E_{NN} = n_{NN}\varepsilon_{NN} \quad (4)$$

where n_{PP}, n_{PN}, and n_{NN} are the numbers of nearest-neighbor monomer–monomer, monomer–particle, and particle–particle, respectively. Here, we set the interactions $\varepsilon_{PP} = \varepsilon_{NN} = 0.63$ and $\varepsilon_{PN} = -0.63$. The value 0.63 is chosen in the way that there is a critical concentration, below which PEs will not collapse directly. As is known, the electrostatic interaction is inversely proportional to the distance r, which indicates the long-range interaction. Here, the cutoff distance of $r_C = \sqrt{5}$ is selected instead of $r_C = \sqrt{2}$ used in the previous work,[22] which would make the results more precise. Here, we aim at studying the effects induced by the magnetic field. Therefore, strong screening of electrostatic interactions actually is assumed, and a simple model for electrostatic interactions is adopted. The cutoff distance of $r_C = \sqrt{5}$ in the calculations of magnetic dipole–dipole interactions does not affect the relation between the applied magnetic field and the statistical properties of system. More detailed discussions about the interactions are included in the Ref. 22.

Our Monte Carlo study is based on the "single-site bond fluctuation model" initiated by Carmesin and Kremer.[29] The simulation is performed in a cubic box of 64 × 64 × 64 Monte Carlo size, with periodic boundary conditions applied in x, y, and z directions. Although the periodical boundary condition is adopted to mimic a practical system, the size effect in simulation may exist. To avoid the finite-size effect, some comparative simulations for different chain lengths (N = 100, 200) have been carried out in a 32 × 32 × 32 Monte Carlo box with the same periodic boundary conditions. Similar results are obtained. It is generally acknowledged that the boundary must be chosen to be at least more than the double gyration radius. In view of the cost of CPU time, the 64 × 64 × 64 Monte Carlo box is selected and the case of N = 300 is also considered. The model system includes 8 N-bond polymer chains and $M(M = 8 \times (N + 1))$ magnetic particles. A particle occupies one lattice site as well as a monomer. Here, the monomer stands for a cluster of real chemical monomers. The excluded volume is performed by forbidding double occupancy. A polymer monomer or a magnetic particle is chosen to move at random. The magnetic moment vector is designed to be reoriented at random even if the chosen particle fails to move. The classical Metropolis scheme is used to sample efficiently the configurational space. The time unit (1MCS), Monte Carlo step, means that each monomer or each particle has one trial to move on average. The annealing procedure is adopted to quickly achieve the equilibrium state. To ensure proper sampling of the conformational space, 10 independent Monte Carlo simulation runs are carried out. Each of the runs is consisted of about 4 × 10^8 MCSs, and the statistical properties are averaged over 15,000 samples after 2 × 10^8 MCSs each run.

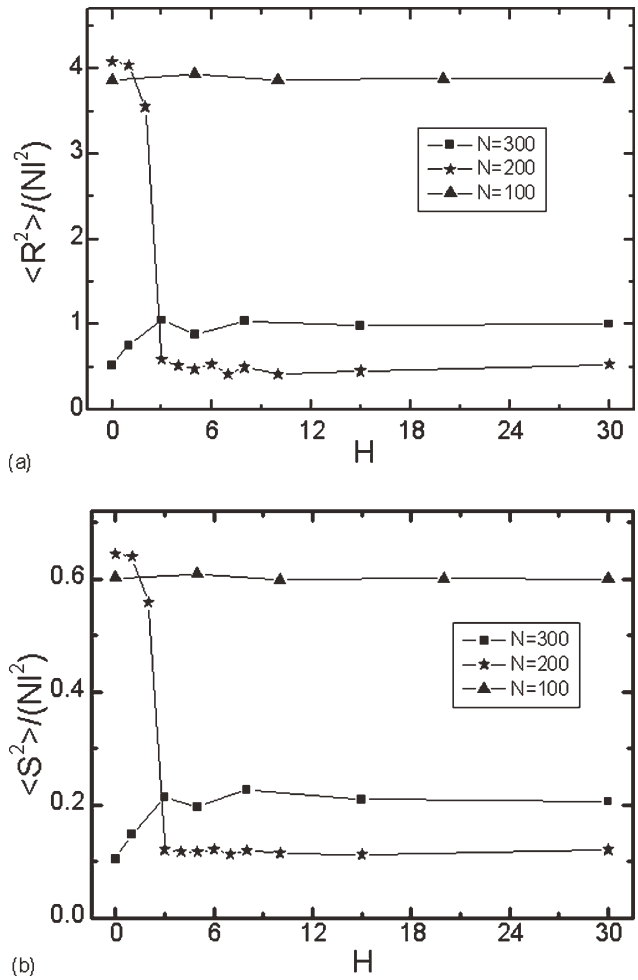

Figure 1 The characteristic ratios as a function of the applied magnetic field H for different chain lengths N: (a) $<R^2>/(Nl^2)$, (b) $<S^2>/(Nl^2)$.

RESULTS AND DISCUSSION

Coil-globule conformational transition of polyelectrolytes

We describe the polymer size by means of the characteristic ratio of mean-square end-to-end distance $<R^2>/(Nl^2)$, where $l = (1 + 2\sqrt{2})/3$ is chosen as the mean bond length in three dimensions. As is depicted in Figure 1(a), the characteristic ratios $<R^2>/(Nl^2)$ for N = 100 remain unchanged for all magnetic fields. However, for N = 200, the characteristic ratio shows no considerable change at small magnetic fields (H = 1, 2), then followed by a sudden decrease at H = 3. Afterward, it remains basically unchanged. In Figure 1(b), the characteristic

ratio of mean-square gyration radius $<S^2>/(Nl^2)$ is used to characterize the tightness of intrachain clusters. The results shown in Figure 1(b) are remarkably similar to that in Figure 1(a). For $N = 100$, the polymer chain has a stretched chain conformation. It can be inferred that there are strong intrachain electrostatic repulsions and weak attractions between monomers and particles, because the number of magnetic particles inside the pervaded volume of the coil is small. However, for $N = 300$ as shown in Figure 1(a,b), the chain collapses initially in the absence of magnetic field H and swells slightly with increasing H. It can be concluded that the electrostatic attraction between monomers and particles induces the initial collapse of charged polymer with $N = 300$. Then, with the increasing of magnetic field H, the collapsed structure is elongated slightly, which is attributed to the competition between the electrostatic attractions and magnetic dipole–dipole interactions. For the case of $N = 200$, the chain collapses rapidly with increasing the magnetic field H. This behavior could be explained by the fact that the potential barrier between the two conformational states can be overcome through the field–particle interactions. To be specific, the magnetic moment vector prefers to turning to the external field direction. The higher is the magnetic field H, the more possibility it does. Therefore, the magnetic particles near PEs are able to aggregate near polymer monomers due to the magnetic dipole–dipole interactions. Meanwhile, the PEs and magnetic particles attract each other to be gathered, because the electrostatic repulsion between particles is largely counterbalanced by magnetic dipole–dipole interactions. Finally, the PEs and magnetic particles are surrounded by each other in some way, leading to PEs collapse into some kinds of globule states. PEs and particles are gathered at the cost of conformational entropy of PEs and translational entropy of particles. On the whole, the role of energy–entropy balance is manifested. In a word, for $N = 100$ and $N = 300$, the phases are dominated by the entropy and energy, respectively. For the case of $N = 200$, the energy gain coming from the magnetic dipole–dipole interactions at large magnetic fields suffices to offset the entropy loss to the extent, and therefore, the conformational transition is triggered.

The shape of the polymer conformation is characterized by using the shape factor, $<\delta^*>$, defined as[32]

$$< \delta* >= 1 - 3 < \frac{L_1^2L_2^2 + L_1^2L_3^3 + L_2^2L_3^2}{L_1^2 + L_2^2 + L_3^2} > \qquad (5)$$

where L_1^2, L_2^2, and L_3^2 represent the eigenvalues of the radius of gyration tensor, respectively. $<\delta^*>$ ranges from 0 for purely spherical chains to 1 for rod-shape chains. As is exhibited in Figure 2, the conformation

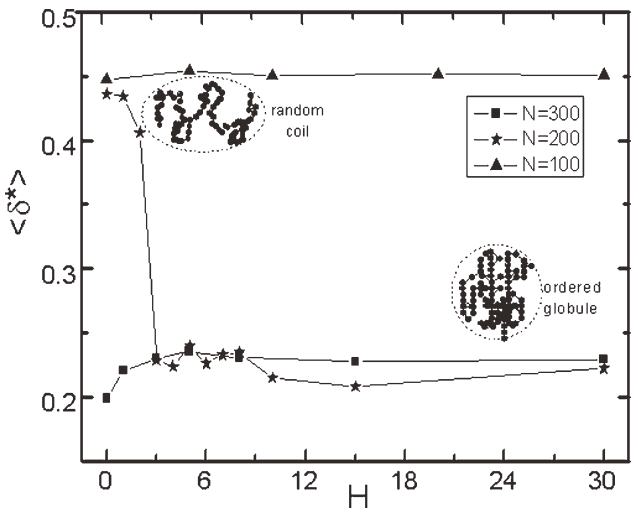

Figure 2 The shape factor $<\delta^*>$ as a function of the applied magnetic field H. The conformational transition from the random coil state to the globule state is shown in the inset.

shape for $N = 100$ is almost an ellipsoidal coil for all magnetic fields. On the contrary, the polymer chain for $N = 300$ is nearly globule-like in the absence of the magnetic field and then swells slightly with increasing the magnetic field strength H. For $N = 200$, the imposed magnetic field greatly influences the shape of polymer chain, leading to the conformational transition from a coil to nearly a globule. The transition is favored by the energy of system. This may be explained by the fact that the magnetic field induces the magnetic particles induced to rearrange in strings along the field direction, to minimize the global energy of system. Meanwhile, the PE chains tend to encompass the monomers as much as possible. As a result, the PE chains are stretched perpendicular to the z-axis. For a good visual presentation, in Figure 3, we also present two typical snapshots of the system with $N = 200$ under different magnetic fields. As shown in Figure 3(a), it is obvious that the magnetic particles and polymers are uniformly distributed in the absence of the external magnetic field ($H = 0$) and the polymer conformations are coil-like. However, when H equals to 3, there are about four ordered aggregates shown in Figure 3(b).

The heat capacity[33] is proportional to the variance of the energy of system $D(E)$ expressed as follows:

$$D(E) =< E^2 > - < E >^2 \qquad (6)$$

Thus, $D(E)$ can be used to characterize the structural phase transition. As shown in Figure 4, it is obvious that there is a peak appearing at the critical point of $H_c = 3$ for $N = 200$. With increasing the magnetic field H, the value of $D(E)$ is sharply improved at $H_c = 3$, then followed by a gradual decrease, which is manifested as a mirror image of the typical λ-shape

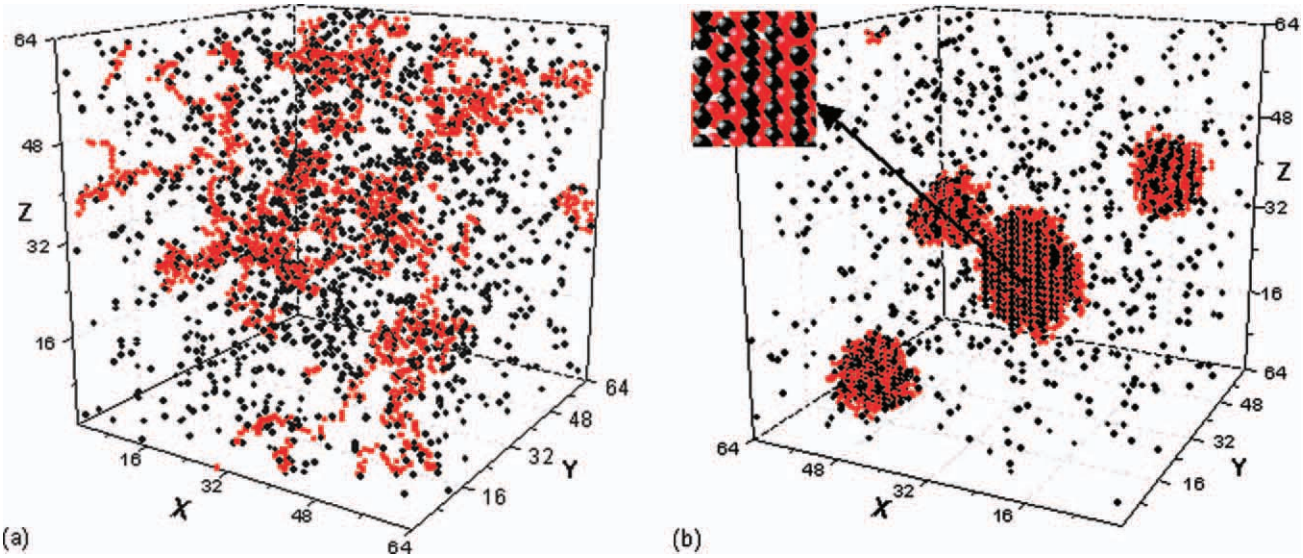

Figure 3 Snapshots of the systems for the cases $H = 0$ (a) and $H = 30$ (b), respectively. A drawing of partial enlargement is shown in the upper left corner and chain length is $N = 200$. Black and red spheres correspond to magnetic particles and polymer monomers, respectively. [Color figure can be viewed in the online issue, which is available at wileyonlinelibrary.com.]

anomaly.[34] Combined with the above results, such curve characteristics is considered as the disorder–order transition of systems. This observation suggests a second-order transition, which here corresponds to the coil-globule conformational transition. Moreover, the error bars are added for different chain lengths. For $N = 200$, the point $H = 2$ seems to be abnormal. As the critical point H_c is approached from $H = 0$, the conformational fluctuations of PEs and the specific heat fluctuations become very large. At this time, the algorithm fails to sample phase space efficiently. This phenomenon is widely considered as "critical slowing down."[35] In a word, the big error at $H = 2$ is acceptable, considering that it does not affect the characterization of the transition.

The system energy E is used to further elucidate the coil-globule transition, where E includes the electrostatic interactions E_e (E_{PP}, E_{NN}, and E_{PN}) and magnetic interactions E_m (E_D and E_H), which have been defined above, respectively. As shown in Figure 5, when the applied magnetic field H increases from 0 to 1, E_H decreases a little because magnetic moment vectors are partly oriented to the field direction. As the applied field is increased to $H = 2$, appreciable changes in energy are observed. The decrease in E_{PN} indicates that there is a little increase in the magnetic particle density near PEs, which contract a bit according to the slight increase in E_{PP}. Therefore, the slight decrease in E_D and increase in E_{NN} result from the magnetic particles near PEs. The sum of E_{NN}, E_{PN}, E_{PP}, and E_D is well below 0, approximately -0.41, where E_D contributes a little. When H is increased from 2 to 3, this case is quite clear for considerable or even sharp changes are seen in Figure 5. The magnetic dipole–dipole interaction E_D changes obviously, although the value of E_D is lower than that of electrostatic interaction E_e. Above $H = 3$, the values of all energy components do not vary with the magnetic field. It means that the system approaches the point of magnetization saturation, where the magnetic moments of particles are basically oriented to the direction of the magnetic field. Therefore, with the further increase of magnetic field H, the energy gain E_m (E_D and E_H) merely comes from the field–particle interactions. Meanwhile, the values of E_{PP}, E_{NN}, and E_{PN} remain unchanged, indicating the structures of aggregates

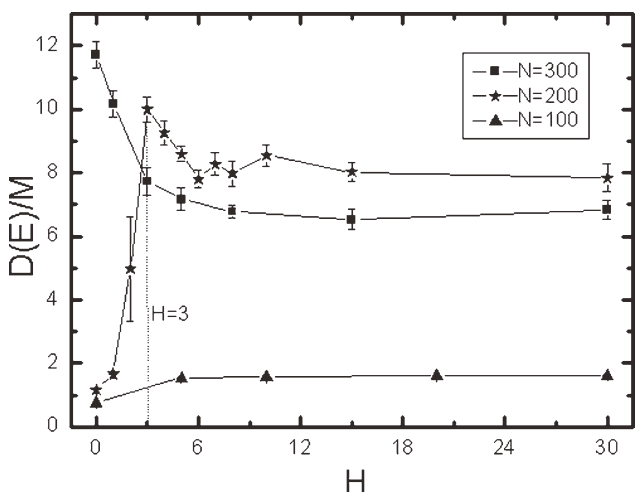

Figure 4 The variance $D(E)$ of the energy per magnetic particle as a function of the applied field H for different chain lengths.

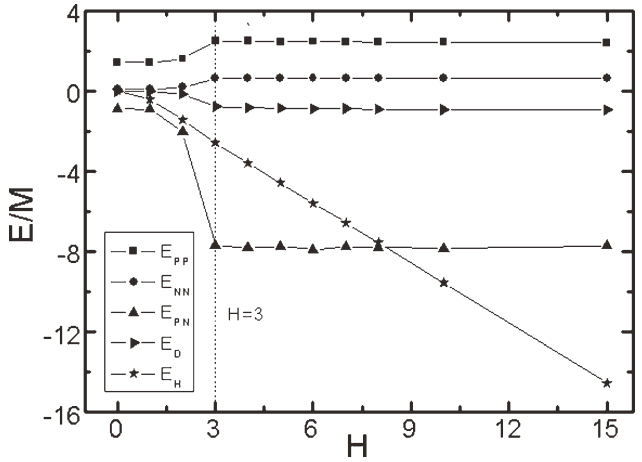

Figure 5 The average energy per monomer (or magnetic particle) E/M as a function of the applied magnetic field H for $N = 200$. E_{PP}, E_{NN}, and E_{PN} represent the electrostatic interactions, and E_D and E_H represent magnetic interactions.

are relatively stable. The sum of E_{PP} and E_{NN} can be used to show whether the string-like structures[22] are stable or not in energy. Similarly, the sum of E_{NN}, E_{PN}, E_{PP}, and E_D reveals the stability of aggregates to some extent. According to the above analysis, some conclusions can be summarized as follows: first, PE chains aggregate magnetic particles during the process of collapsing. In other words, PEs' collapse is conjugated to the particle adsorption. Second, the string-like structures of magnetic particles are energetically favored, because the sum of E_{PP} and E_{NN} is obviously less than 0. Finally, it is the magnetic dipole–dipole interaction that triggers the conformational transition by offsetting electrostatic repulsion to increase the density of the magnetic particles near PEs. Meanwhile, the electrostatic interaction plays a major role in stabilizing new phase, which is clearly shown in the case of $N = 300$.

Statistical properties of magnetic nanoparticles

The magnetic susceptibility is the degree of magnetization of a material in response to an applied magnetic field. To characterize the magnetization properties of nanoparticles, the magnetic susceptibility is defined as follows[33]:

$$\chi = \frac{1}{kTM}(< m_z^2 > - < m_z >^2) \tag{7}$$

where m_z is the mean magnetization of system in the z-axis direction (i.e., the applied magnetic field direction), M is the total number of magnetic particles, and $< >$ denotes an average over all possible states of the system. As shown in Figure 6, the initial value of χ is ~ 0.5, revealing that the dipole–dipole interactions among particles are so weak that the magnetic moments are uniformly distributed in all directions. It can be interpreted by

$$\chi = \frac{1}{kTM}\left(M\int_0^\pi m_0^2\cos^2\theta f(\theta)d\theta - \left(M\int_0^\pi m_0\cos\theta f(\theta)d\theta\right)^2\right)$$
$$= \int_0^\pi \frac{1}{\pi}\cos^2\theta d\theta - 0 = 0.5 \tag{8}$$

provided that the m_z has a uniform distribution in the range from 0 to π, i.e., the probability density $f(\theta)$ of $m_z (m_z = m_0 \cos\theta)$ is $1/\pi$. As clearly shown in Figure 6, the value of χ decreases monotonically with the applied magnetic field H. First, χ decreases rapidly with the magnetic field increased from $H = 0$ to $H = 3$. After the critical point $H = 3$, the value of χ is slightly decreased and finally stabilized. It indicates that the saturation magnetization of system has been approached, and then the magnetic dipole–dipole interactions make no appreciable change (see E_{NN} in Fig. 5) and the new phase is stabilized.

Pair correlation function $g(r)$ is often used to investigate the distribution of particles. In view of the anisotropy resulting from the magnetic field, $g_{xy}(r)$ and $g_z(r)$ are considered, respectively, which are defined as[22]

$$g_{xy}(r) = \frac{V}{M^2}N_{xy} \tag{9}$$

and

$$g_z(r) = \frac{V}{M^2}N_z \tag{10}$$

where V denotes the system volume, N_z is the number of pairs whose distance is r along the z-axis, and

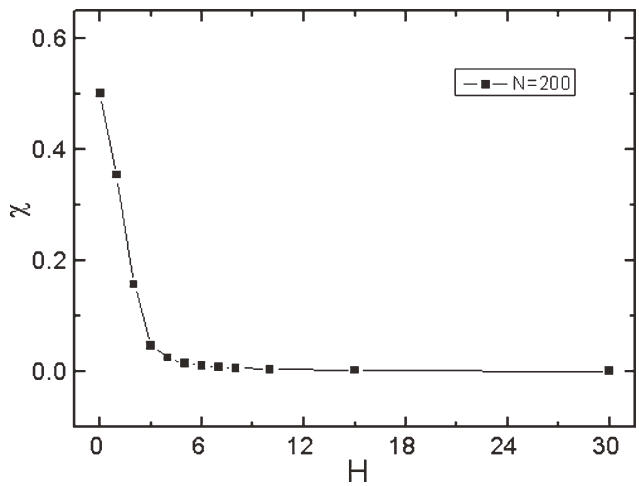

Figure 6 The magnetic susceptibility χ as a function of the applied magnetic field H.

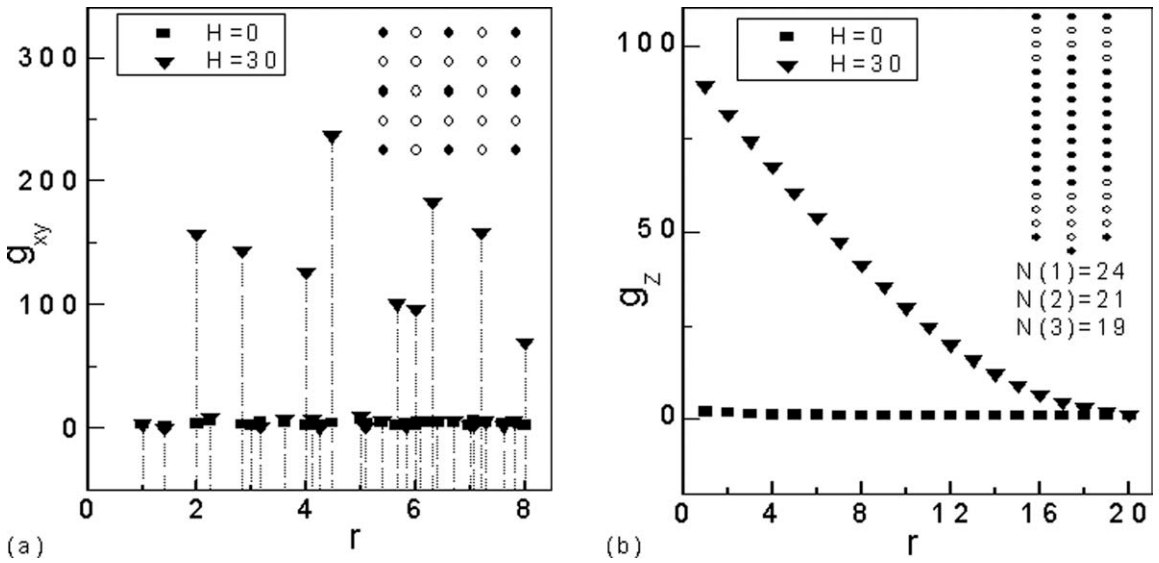

Figure 7 The pair correlation functions g_{xy} (*r*) (a) and g_z (*r*) (b) as a function of the distance *r* between magnetic particles for $H = 0$ and 30. Two possible arrangements are presented in the inset, and filled circles represent magnetic particles.

N_{xy} the number of pairs whose distance is *r* in the *xy*-plane. As g_{xy} (*r*) shown in Figure 7(a), in the absence of the magnetic field ($H = 0$), the probabilities of finding particles separated from each other for different distances *r* do not differ much. It indicates that the magnetic particles are uniformly distributed in the *xy*-plane, which has also been displayed by the magnetic susceptibility χ in Figure 6. However, under a large magnetic field of $H = 30$ as shown in Figure 3(b), some aggregates of magnetic particles and polymers are observed. The distribution of magnetic particles within aggregates exhibits a kind of short-range order, which is supported by the fluctuation in g_{xy} (*r*) function shown in Figure 7(a). The most possible arrangement seems like a square lattice with 2 lattice units, as its own lattice unit [see the inset in Fig. 7(a)] according to the points with maximum values $(r = 2\sqrt{i^2 + j^2}; i, j = 0, 1, 2, 3, 4, \cdots)$. Therefore, with increasing the distance *r*, the maximum values decrease considerably and deviate from the theoretical values of ideal square lattice. Similarly, as shown in Figure 7(b), for $H = 0$, the magnetic particles are randomly distributed along the *z*-axis, whereas for $H = 30$ the values of g_z (*r*) decrease regularly with increasing the distance *r*. It means that the short-range order arrangement of magnetic particles in *z*-axis direction is induced by the large magnetic field. To be specific, a number of string-like structures[36] are formed. That is why the numbers of pairs for shorter distances is always greater than that for longer distances. Additionally, these string-like structures are displayed in the inset of Figure 7(b). Finally, we investigate the properties of string-like structures by calculating the average length $<L_Z>$, which is defined as the length of magnetic particles arranged along the *z*-axis. As shown in Figure 8, for $N = 100$, the values of $<L_Z>$ show no significant difference with and without the applied magnetic field. For $N = 200$, the values of $<L_Z>$ are a little greater than 1 when $H = 0$ and 1. This is because magnetic particles collide with each other by accident. When *H* equals to 2, the value of $<L_Z>$ is ~ 2, which indicates that the average density of magnetic particles near the polymers increase slightly, and the short string-like structures are formed with the help of the electrostatic attraction between monomers and particles. With a further increase in magnetic field *H*, the magnetic dipole–dipole interactions will be strengthened, and the local density of magnetic particles near PEs will increase. Then, there is a sudden and sharp increase

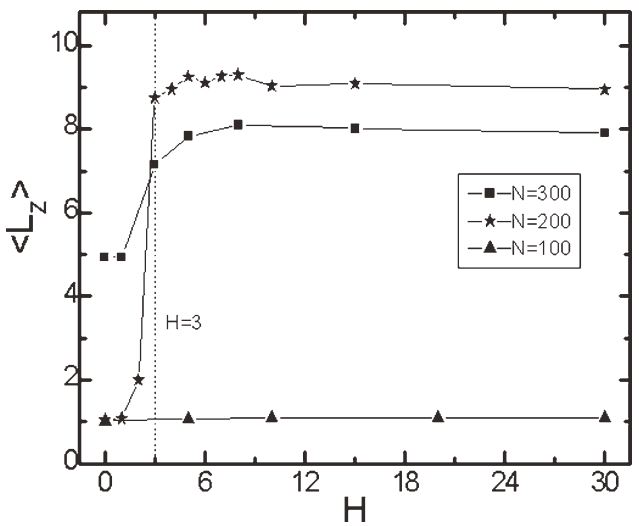

Figure 8 The average length $<L_Z>$ of string-like structures of magnetic particles as a function of the applied magnetic field *H* with different chain lengths.

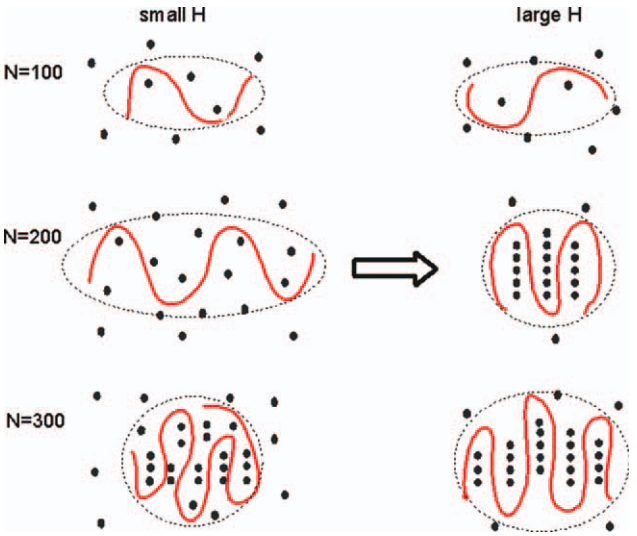

Figure 9 The schematic conformations of PEs at small and high magnetic fields for different chain lengths. [Color figure can be viewed in the online issue, which is available at wileyonlinelibrary.com.]

in $<L_Z>$ at the critical point $H = 3$, suggesting that the long string-like structures are formed after the collapse of PEs. Finally, the increase of magnetic field H does not make any essential variation, only with small fluctuations in $<L_Z>$. In this case, it is obvious that energy gain is preferred to entropy loss. Different from the case of $N = 200$, the value of $<L_Z>$ for $N = 300$ approximately equals to 5 without magnetic field ($H = 0$). This can be interpreted by the fact that the spontaneous magnetic moments induce each other within a short distance, due to the collapse of PEs resulting from the electrostatic interactions. With increasing the magnetic field H, the value of $<L_Z>$ is rapidly improved to 8, but always less than that for $N = 200$. This phenomenon reveals that the ratio of the number of magnetic particles in aggregates to the number of string-like structures for $N = 300$ is smaller than that for $N = 200$. It can be attributed to the fact that as the chain length increases, such as increased from $N = 200$ to 300 , the magnetic particles tend to encircle aggregates rather than increase the length of string structures. In this way, the electrostatic attractive energy and, thus, global energy of system are favored.

Finally, Figure 9 schematically shows the induced coil-globule transition process for different chain lengths. For $N = 100$, the PE chains have no conformational transition with the increase of magnetic field, because energy gain is not preferred to entropy loss. In contrast, for $N = 300$, at small magnetic fields, the PE chains are in a globule state and short string-like structures within the aggregates are formed. This is because the system is too dense and the electrostatic interactions dominate the phase. At high magnetic fields, magnetic dipole–dipole interactions among magnetic particles seem to attract each other and largely offset the electrostatic repulsion between particles. Thus, the energetically favorable string-like structures are strengthened and lengthened. To minimize the globule energy of system, the PE chains have to encircle particles and then are stretched in the xy-plane. Surprisingly, for $N = 200$ with the increasing of magnetic field H, there is a conformational transition from coil state to globule state. At small magnetic fields, the PE chains are in a coil state. As H is increased, the magnetic dipole–dipole interactions begin to counterbalance the electrostatic repulsion between magnetic particles, and the local density of particles near the PE chains increases. At the high magnetic fields, energy gain suffices to defeat entropy loss, and then the PE chains collapse with the adequate adsorption of magnetic particles.

CONCLUSIONS

The system composed of PEs and magnetic nanoparticles with opposite charges is investigated by means of Monte Carlo simulations. Polymer chains are modeled as sequences of identical monomers, whose positions are restricted to the simple cubic lattice. We describe the mean dimensions of PEs in terms of the characteristic ratios of mean-square end-to-end distance and gyration radius. The shape factor is used to characterize the shape conformation of PE chains. For chain length $N = 200$, the conformation changes from a coil state to a globule state with increasing the applied magnetic field. For $N = 100$ and $N = 300$, the phases are dominated by the entropy and energy, respectively. On the whole, the role of energy–entropy balance is reflected by the cases for different chain lengths. The thermodynamic nature of the transition is characterized by a typical λ anomaly. By analyzing the system energy, at high magnetic fields, the collapse of PEs for $N = 200$ is attributed to the fact that the electrostatic repulsion among the magnetic particles near PEs is largely offset by the magnetic dipole–dipole interactions. During the transition process, PEs collapse by collecting the abundant magnetic particles. The magnetic susceptibility of particles is a monotonic decreasing function of the applied magnetic field, which indicates that the spatial arrangement of magnetic particles is greatly affected by the imposed magnetic field. There is a string-like arrangement along the magnetic field and a square lattice-like arrangement perpendicular to the magnetic field. For $N = 200$, with the increasing of applied magnetic fields, the average length of string-like structures is improved and stabilized finally. For $N = 300$, spontaneous magnetization plays a major role in the string-like arrangement in the absence of magnetic field, so the

average length of string-like structures also increases significantly with the applied field. However, the maximum average length of $N = 200$ is greater than that of $N = 300$, which is attributed to the energetical favorableness. Based on the simplified simulation model, more details such as counterions will be taken into account in our future work.

References

1. Nishio, I.; Sun, S. T.; Swislow, G.; Tanaka, T. Nature 1979, 281, 208.
2. Ivanov, V. A.; Paul, W.; Binder, K. J Chem Phys 1998, 109, 5659.
3. Mishra, P. K.; Kumar, S. J Chem Phys 2004, 121, 8642.
4. Rissanou, A. N.; Anastasiadis, S. H.; Bitsanis, I. A. J Polym Sci Part B: Polym Phys 2009, 47, 2462.
5. Gunari, N.; Balazs, A. C.; Walker, G. C. J Am Chem Soc 2007, 129, 10046.
6. Shepherd, J.; Sarker, P.; Swindells, K.; Douglas, I.; MacNeil, S.; Swanson, L.; Rimmer, S. J Am Chem Soc 2010, 132, 1736.
7. Tanaka, F.; Koga, T.; Kojima, H.; Winnik, F. O. M. Macromolecules 2009, 42, 1321.
8. Walter, R.; Rička, J.; Quellet, C.; Nyffenegger, R.; Binkert, T. Macromolecules 1996, 29, 4019.
9. Zhou, K.; Lu, Y.; Li, J.; Shen, L.; Zhang, G.; Xie, Z.; Wu, C. Macromolecules 2008, 41, 8927.
10. Sear, R. P. Phys Rev E 1998, 58, 724.
11. Kamata, K.; Araki, T.; Tanaka, H. Phys Rev Lett 2009, 102, 108303.
12. Polson, J. M.; Opps, S. B.; Abou Risk, N. J Chem Phys 2009, 130, 244902.
13. Baysal, B. M.; Karasz, F. E. Macromol Theor Simul 2003, 12, 627.
14. de Gennes, P. C. Scaling Concepts in Polymer Physics; Cornell University Press: Ithaca, 1979.
15. Rubinstein, M.; Colby, R. H. Polymer Physics; Oxford University Press: London, 2003.
16. Brilliantov, N.; Kuznetsov, D.; Klein, R. Phys Rev Lett 1998, 81, 1433.
17. Hsiao, P.-Y.; Luijten, E. Phys Rev Lett 2006, 97, 148301.
18. Loh, P.; Deen, G. R.; Vollmer, D.; Fischer, K.; Schmidt, M.; Kundagrami, A.; Muthukumar, M. Macromolecules 2008, 41, 9352.
19. Panwar, A. S.; Kelly, M. A.; Chakrabarti, B.; Muthukumar, M. Arxiv Prepr arXiv:0905.4524v1.
20. Cherstvy, A. G. J Phys Chem B 2010, 114, 5241.
21. Kundagrami, A.; Muthukumar, M. Macromolecules 2010, 43, 2574.
22. Ye, Y.; Pan, Z.; Zhang, L.; He, L.; Xia, A.; Liang, H. J Polym Sci Part B: Polym Phys 2010, 48, 1873.
23. Choi, W. S.; Koo, H. Y.; Kim, J. Y.; Huck, W. T. S. Adv Mater 2008, 20, 4504.
24. Mackay, M. E.; Tuteja, A.; Duxbury, P. M.; Hawker, C. J.; Van Horn, B.; Guan, Z.; Chen, G.; Krishnan, R. S. Science 2006, 311, 1740.
25. Shchukin, D. G.; Sukhorukov, G. B. Adv Mater 2004, 16, 671.
26. Shchukin, D. G.; Radtchenko, I. L.; Sukhorukov, G. B. J Phys Chem B 2003, 107, 86.
27. Mayya, K. S.; Schoeler, B.; Caruso, F. Adv Funct Mater 2003, 13, 183.
28. Joly, S.; Kane, R.; Radzilowski, L.; Wang, T.; Wu, A.; Cohen, R. E.; Thomas, E. L.; Rubner, M. F. Langmuir 2000, 16, 1354.
29. Carmesin, I.; Kremer, K. Macromolecules 1988, 21, 2819.
30. Sadovoy, A. V.; Bratashov, D. N.; Yashchenok, A. M.; Svenskaya, Y. I.; Sukhorukov, G. B.; Gorin, D. A. Tech Phys Lett 2010, 36, 88.
31. Hu, S. H.; Tsai, C. H.; Liao, C. F.; Liu, D. M.; Chen, S. Y. Langmuir 2008, 24, 11811.
32. Jagodzinski, O.; Eisenriegler, E.; Kremer, K. J Phys I 1992, 2, 2243.
33. Konstantinova, E. J Magn Magn Mater 2008, 320, 2721.
34. Fujimoto M. The Physics of Structural Phase Transitions; Springer Press: New York, 2005, Chapter 1.
35. Binder, K.; Heermann, D. W. Monte Carlo Simulations in Statistical Physics: An Introduction; Springer Press: Berlin, 1988; Chapter 4.
36. Satoh, A. J Colloid Interface Sci 1996, 181, 422.